Inorganica Chimica Acta 363 (2010) 3131–3138

Contents lists available at ScienceDirect

Inorganica Chimica Acta

journal homepage: www.elsevier.com/locate/ica

Iron(III) complexes using NNS reduced Schiff bases and NNOS coordinating tetradentate ligands: Synthesis, structure and catecholase activity

Reena Singh, Atanu Banerjee, Kajal Krishna Rajak *

Inorganic Chemistry Section, Department of Chemistry, Jadavpur University, Kolkata 700032, India

A R T I C L E   I N F O

Article history:
Received 27 January 2010
Received in revised form 12 May 2010
Accepted 14 May 2010
Available online 24 May 2010

Dedicated to Animesh Chakravorty

Keywords:
Iron(III)
NNS and NNOS ligands
Structure
Catecholase activity

ABSTRACT

The orange–red colored complexes of the type $[Fe(L_{SB})Cl_3]$, **1**, have been synthesized in excellent yields by reacting $FeCl_3{\cdot}6H_2O$ with L_{SB} in methanol. Here, L_{SB} is (2-(ethylthio)-*N*-(pyridin-2-ylmethyl)ethanamine), ($L_{SB}{}^1$) and (2-(benzylthio)-*N*-(pyridin-2-ylmethyl)ethanamine) ($L_{SB}{}^2$). Similarly, $FeCl_3{\cdot}6H_2O$ reacted with 2-(((2-(ethylthio) ethyl) (pyridin-2-ylmethyl)amino)methyl)phenol (HL^1), 2-(((2-(ethylthio)ethyl)(pyridin-2 ylmethyl)amino)methyl)-4-nitrophenol (HL^2), 4-chloro-2-(((2-(ethylthio)ethyl)(pyridin-2-ylmethyl)-amino)methyl)phenol (HL^3), 2-(((2-(benzylthio)ethyl)(pyridin-2-ylmethyl) amino)methyl)phenol (HL^4), 2-(((2-(benzylthio)ethyl)(pyridin-2-ylmethyl)amino)methyl) -4-nitrophenol (HL^5), and 4-chloro-2-(((2-(benzylthio)ethyl)(pyridin-2-ylmethyl)amino) methyl)phenol (HL^6) to give dichloro complexes of the type $[Fe(L)Cl_2]$, **2**. The solid and solution structure of the complexes, as well as their properties, were probed using X-ray diffraction, spectroscopic and electrochemical methods. The Mössbauer spectral study at 80 K for complexes reveals the existence of (III) oxidation state and high-spin state of the metal center in the complex. Dioxygenase activity of the complexes has been studied and both **1** and **2** have been found to display the intradiol-cleaving pathway. However, no extradiol cleavage products have been isolated.

1. Introduction

The chemistry of mononuclear iron(III) complexes has aroused considerable interest as iron has been found in active sites of the large number of metalloenzymes [1–11]. Among them, the catecholase dioxygenases are non-heme iron containing enzymes, mainly found in soil bacteria, and play a key role in biodegradation of naturally occurring aromatic 1,2-dihydroxy compound to aliphatic product by oxidative ring cleavage [12,13]. The catechol dioxygenases can be subdivided into two classes [11,14,15]. The first one is the intradiol cleaving enzymes containing a non-heme iron(III) co-factor that catalyze a C_1–C_2 bond between the two catechol oxygen atoms giving muconic acid and the second one is the extradiol dioxygenases which utilizes the non-heme iron(II) that catalyze either C_2–C_3 or C_1–C_6 bond cleavage of catechol yielding 2-hydroxy muconic semialdehyde (Scheme 1).

The X-ray structure of intradiol cleaving enzyme protocatechuate 3,4-dioxygenase from *Pseudomonas putida* reveals that, in the active site of the enzyme the iron(III) center is coordinated by two nitrogen atoms from histidine residue, two oxygen atoms from tyrosinase moiety and a solvent derived hydroxide ligand in a distorted trigonal geometry arrangement (Scheme 2(A)) [16,17]. On the other hand, in the active sites of the extradiol cleaving enzyme contain, Fe(II) center in which Fe(II) center is bonded with histidine residue, one glutamic acid residue and two water molecules forming a distorted square pyramid geometry (Scheme 2B) [18,19]. A considerable number of mononuclear Fe(III) complexes of nitrogen, carboxylate and phenolate donor have been synthesized as functional model to explore their dioxygenase activity towards the different catechol substrates as well as to investigate the mechanism of catechol oxidation [20–31]. Despite the large number of Fe(III) complexes with O,N coordinating ligands discovered so far, the chemistry of mononuclear Fe(III) complexes with thioether ligands is still restricted and much remains to be done. A very few Fe(III) thioether complexes have been isolated and characterized [32–37] and the hardness of iron(III) has been probably found to be responsible for lesser known Fe^{III}–S (thioether) species in pure form. This has prompted us to undertake the task of synthesis of Fe(III) complexes incorporating *N*,*O*,*S* coordinating ligands and to understand how the small variation in the ligand, modulate the details of molecular structure as well as their catecholase activity.

Here, we describe the synthesis of two families of mononuclear Fe(III) complexes of types $[Fe^{III}(L_{SB})Cl_3]$, **1** and $[Fe^{III}(L)Cl_2]$, **2** using conformationally labile *N*,*N*,*S*-coordinating tridentate reduced Schiff base ligands and *N*,*N*,*O*,*S*-donating tetradentate ligands, respectively. The X-ray structures of two representative complexes have been determined. The spectral and electrochemical behaviors of the complexes have been described. The catecholase activity of the complexes has also been studied.

---

* Corresponding author.
E-mail address: kkrajak@chemistry.jdvu.ac.in (K.K. Rajak).

0020-1693/$ - see front matter © 2010 Elsevier B.V. All rights reserved.
doi:10.1016/j.ica.2010.05.027

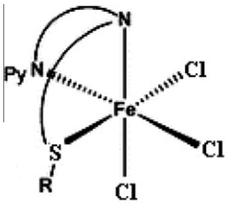

1

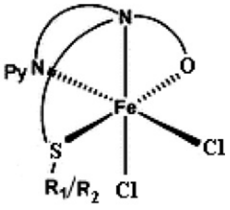

2

2. Results and discussion

2.1. Syntheses

The two tridentate (*N*,*N*,*S*) reduced Schiff bases L_{SB}^1 and L_{SB}^2 (general abbreviation, L_{SB}) and six tetradentate (*N*,*N*,*O*,*S*) HL^1–HL^6 (generally written as HL) ligands are used (Chart 1) in the present work and the types of complexes synthesized are listed in Chart 2.

The stoichiometric reaction of $FeCl_3{\cdot}6H_2O$ with L_{SB} in refluxing MeOH afforded the orange–red complexes of general formula $[Fe^{III}(L_{SB})Cl_3]$, **1** in good yields (Eq. (1)).

$$FeCl_3\cdot 6H_2O \xrightarrow[\text{MeOH, reflux (2 h)}]{L_{SB}} \left[Fe^{III}(L_{SB})Cl_3\right] \tag{1}$$

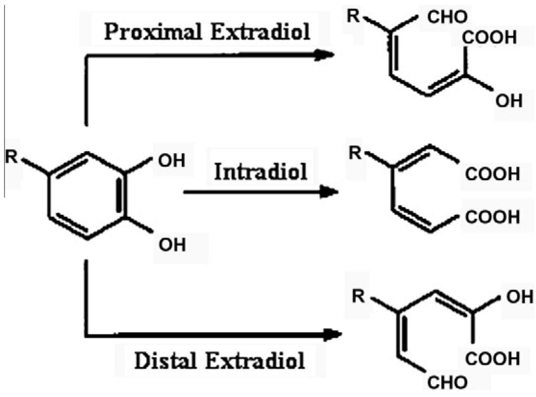

Scheme 1.

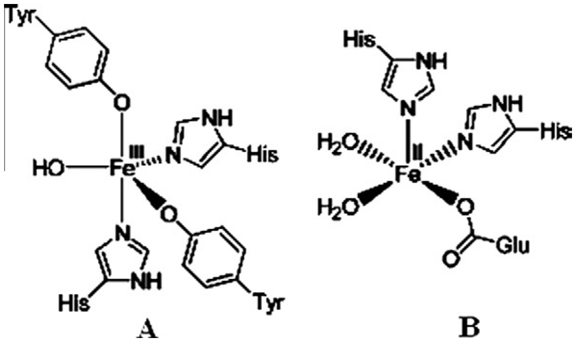

Scheme 2.

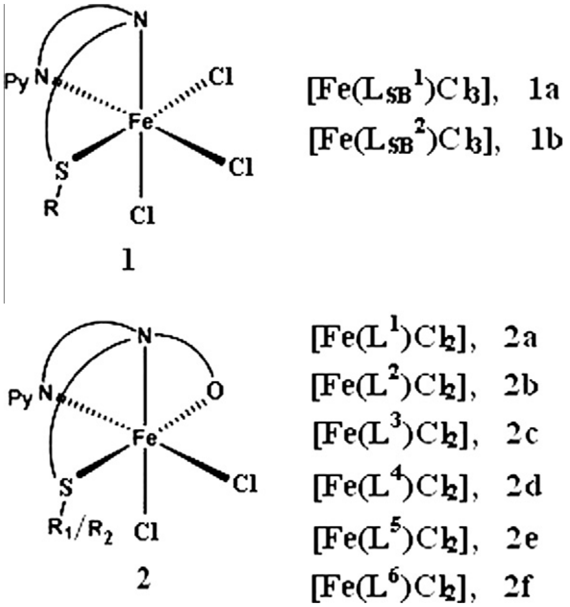

Chart 2.

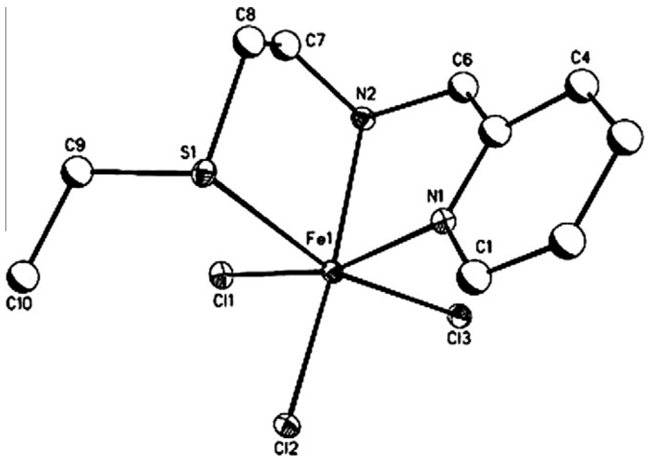

Fig. 1. Molecular view and labeling scheme for selected atoms of $[Fe^{III}(L_{SB}^1)Cl_3]$. All the hydrogen atoms are omitted for clarity.

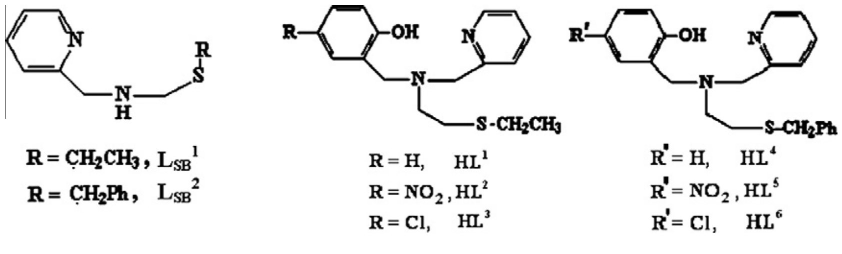

Chart 1.

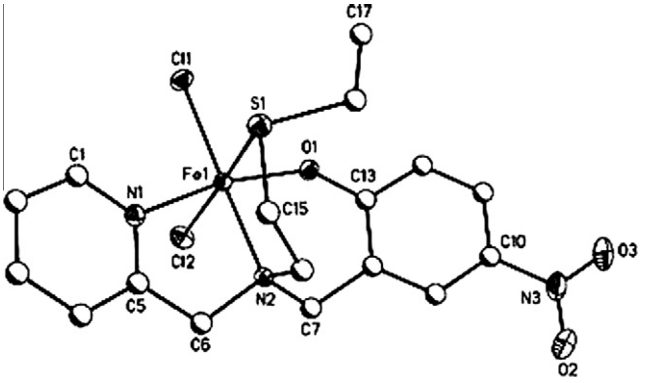

Fig. 2. Molecular view and labeling scheme for selected atoms of $[\mathrm{Fe^{III}}(L^2)Cl_2]$. All the hydrogen atoms are omitted for clarity.

Table 1
Selected bond lengths (Å) and angles (°) for $[\mathrm{Fe^{III}}(L_{SB}{}^1)Cl_3]$.

Distances	
Fe(1)–N(1)	2.181(4)
Fe(1)–N(2)	2.212(4)
Fe(1)–S(1)	2.6280(14)
Fe(1)–Cl(1)	2.2836(14)
Fe(1)–Cl(2)	2.3149(13)
Fe(1)–Cl(3)	2.2930(14)
Angles	
N(1)–Fe(1)–N(2)	76.48(15)
N(1)–Fe(1)–Cl(1)	164.30(12)
N(1)–Fe(1)–Cl(2)	94.17(11)
N(1)–Fe(1)–Cl(3)	88.72(12)
N(1)–Fe(1)–S(1)	77.94(12)
N(2)–Fe(1)–Cl(1)	89.74(11)
N(2)–Fe(1)–Cl(2)	164.90(11)
N(2)–Fe(1)–Cl(3)	89.10(12)
N(2)–Fe(1)–S(1)	79.59(12)
Cl(1)–Fe(1)–Cl(2)	97.64(5)
Cl(1)–Fe(1)–Cl(3)	98.69(5)
Cl(1)–Fe(1)–S(1)	92.36(5)
Cl(2)–Fe(1)–Cl(3)	102.68(5)
Cl(2)–Fe(1)–S(1)	86.94(5)
Cl(3)–Fe(1)–S(1)	164.16(4)

Table 2
Selected bond lengths (Å) and angles (°) for $[\mathrm{Fe^{III}}(L^2)Cl_2]$.

Distances	
Fe(1)–O(1)	1.9060(12)
Fe(1)–N(1)	2.1697(14)
Fe(1)–N(2)	2.2688(13)
Fe(1)–S(1)	2.6761(5)
Fe(1)–Cl(1)	2.2744(5)
Fe(1)–Cl(2)	2.3026(5)
Angles	
O(1)–Fe(1)–N(1)	162.70(5)
O(1)–Fe(1)–N(2)	87.87(5)
O(1)–Fe(1)–S(1)	92.63(4)
O(1)–Fe(1)–Cl(1)	98.21(4)
O(1)–Fe(1)–Cl(2)	97.31(4)
N(1)–Fe(1)–N(2)	75.88(5)
N(1)–Fe(1)–S(1)	78.47(4)
N(1)–Fe(1)–Cl(1)	95.91(4)
N(1)–Fe(1)–Cl(2)	90.12(4)
N(2)–Fe(1)–S(1)	78.45(4)
N(2)–Fe(1)–Cl(1)	163.31(4)
N(2)–Fe(1)–Cl(2)	95.00(4)
S(1)–Fe(1)–Cl(1)	85.727(18)
S(1)–Fe(1)–Cl(2)	167.907(18)
Cl(1)–Fe(1)–Cl(2)	99.58(2)

Table 3
Crystal data and structure refinement parameters for $[\mathrm{Fe^{III}}(L_{SB}{}^1)Cl_3]$, **1a** and $[\mathrm{Fe^{III}}(L^2)Cl_2]$, **2b**.

	1a	**2b**
Formula	$C_{10}H_{16}Cl_3FeN_2S$	$C_{17}H_{20}Cl_2FeN_3O_3S$
Formula weight	358.51	473.17
Crystal system	orthorhombic	monoclinic
Space group	*F2dd*	$P2_1/c$
a (Å)	7.654(2)	20.0756(4)
b (Å)	25.597(7)	7.58790(10)
c (Å)	29.921(8)	13.4287(2)
β (°)	90.00	106.0070(10)
V (Å^3)	5862(3)	1966.30(6)
Z	16	4
D_{calc} (mg m^{-3})	1.929	1.598
μ (mm^{-1})	2.016	1.168
θ (°)	2.09–29.42	1.06–27.73
T (K)	293(2)	293(2)
R_1[a], wR_2[b] [$I > 2\sigma(I)$]	0.0503, 0.1172	0.0255, 0. 0.0716
GOF on F^2	0.956	1.116

[a] $R_1 = \Sigma|F_o| - |F_c|/\Sigma|F_o|$.
[b] $wR_2 = [\Sigma w(F_o^2 - F_c^2)^2/\Sigma w(F_o^2)^2]^{1/2}$.

On the other hand, complexes of the type $[\mathrm{Fe^{III}}(L)Cl_2]$, **2** were obtained as deep blue solid from a reaction of $FeCl_3{\cdot}6H_2O$ with HL in a 1:1 ratio (Eq. (2)).

$$FeCl_3 \cdot 6H_2O \xrightarrow[\text{MeOH, reflux (2 h)}]{\text{HL}} \left[\mathrm{Fe^{III}}(L)Cl_2\right] \qquad (2)$$

The IR and UV–Vis spectral data of the complexes are given in the Experimental Section. The complexes display Fe–S and Fe–Cl stretches near 340 cm^{-1} and 390 cm^{-1}, respectively. The type **2** compounds display [38] Fe–O and C–O stretches in the region 760–770 cm^{-1} and 1270–1300 cm^{-1}, respectively.

All the iron(III) complexes have magnetic moments in the range 5.2–5.8 BM at room temperature which is consistent with a high-spin ferric center.

The complexes were found to be NMR silent in $CDCl_3$ solution at room temperature.

2.2. Crystal structure

The structures of **1a** and **2b** have been determined. Molecular views excluding the hydrogen atoms are shown in Figs. 1 and 2, respectively. The selected bond parameters are given in Tables 1 and 2, respectively. Significant crystal data are given in Table 3.

2.2.1. $[\mathrm{Fe^{III}}(L_{SB}{}^1)Cl_3]$, **1a**

The complex **1a** is a neutral Fe(III) complex in which iron is hexacoordinated with a distorted octahedral geometry. The iron(III) center is facially coordinated by two nitrogen atoms and one sulfur donor atom (N1, N2, S1) of the ligand $L_{SB}{}^1$, and the three chloride ions complete the remaining octahedral sites. The Fe–N_{Py} bond distance (2.18(4) Å) falls in the range of Fe–N_{Py} bond distances [39–47]. As the secondary amine and pyridine nitrogen atoms are sp^3 and sp^2-hybridized, the distances between the iron(III) and secondary amine nitrogen atom (2.210(4)) is expected to be longer than that between the iron(III) and pyridine nitrogen atom. Further, the Fe–S bond is significantly longer than the Fe–N bond due to inability of sterically hindering S–(CH_2CH_3) group to properly orient [22,48, 49–53] itself towards iron(III). The deviation [48] from a perfect octahedral geometry is best illustrated by the S–Fe–Cl3(164.16°), N1–Fe–Cl1(164.30°) and N2–Fe–Cl2(164.90°) bond angles, which markedly deviate from that (180°) of an ideal octahedron. The Fe–$Cl_{equatorial}$ distances (2.293(2) Å) and (2.283(2) Å) are, as expected, shorter than the Fe–Cl_{axial} (2.315(2) Å).

2.2.2. *[$Fe^{III}(L^2)Cl_2$],* **2b**

The complex crystallizes in $P2_1/c$ space group. The molecule has FeN_2OSCl_2 coordination sphere with a distorted octahedral geometry, constituted by two nitrogen atoms, one sulfur, one phenolato oxygen and two chloride ions. The ligand binds in a facial coordination mode in which the amine nitrogen (N2) and chloride (Cl1) ion occupy the axial position whereas the equatorial plane is occupied by S1, N1, Cl2 and O1. The $Fe–N_{py}$ bond length (2.170(2) Å) is shorter than the $Fe–N_{amine}$ bond distance (Fe–N2), (2.269(2) Å), which is expected of the difference in hybridization of nitrogen atoms.

The Fe–O(phenolate) bond is significantly different (Fe–O1, 1.9 Å) but are similar to those reported for six-coordinated iron(III) complexes [54–62]. The phenolate oxygen in the six membered ring has an Fe–O1–C13 bond angle 134.41°, which is higher than the ideal value of 120° for an sp^2 hybridized phenolate oxygen atom indicating that the latter (in-plane p–π orbital) interacts [62] less strongly for a half-filled d_π^* orbital on iron(III). Also the angle is higher than the average Fe–O–C bond angle of ~128.5° observed in other octahedral iron(III) complexes [56–65].

The longer Fe–S (2.676(2) Å) is probably due to the presence of sterically hindering *S-(CH_2CH_3)* group which leads to an improper orientation [22,48,43] of the lone pair orbital on sulfur atom towards the iron(III) orbital. The S–Fe–Cl2 bond angle being 167.91° also deviates significantly from 180°. The Fe–Cl distances (~2.28 Å) are in the same range [52,56,62,64] as those in octahedral iron(III) complexes suggesting that the chloride ions should be labile in solution.

2.3. EPR and Mössbauer spectra

An important requirement of an intradiol catechol dioxygenase model is the high-spin nature of the iron(III) metal center. In this context, the electron paramagnetic resonance (EPR) studies deserve mention. The X-band EPR of the complexes were recorded in frozen solution and exhibits a well resolved EPR signal near $g = 4.1$ typical of a monomeric high-spin Fe(III) center in a distorted octahedral environment [66–71] (Fig. S1). For example, similar EPR spectra were observed for related monomeric high-spin octahedral complexes, namely, [bis(pyridin-2-ylmethyl)amine]$FeCl_3$ [55], ($g = 4.30$), [bis(benzimidazol-2-ylmethyl)amine]$FeCl_3$ [55] ($g = 4.22$), and [4,5-dichloro-1,2-bis(pyridinecarboxamido)benzene]Fe–(NEt_4)Cl_2 [72] ($g = 4.28$).

Table 4
Absorption maxima of bands observed in the UV–Vis spectra of Fe(III) and Fe(III)–catecholate complexes in CH_3CN solution.

λ_{max} (nm) (ε, M^{-1} cm^{-1}) Ligand added Complex	None	H_2DBC
1a	360(4100),310(4475), 240 (10185)	870(2580), 500(1555)
1b	355(2235), 315(2985), 255(9165)	910(2060), 580(1770)
2a	600(2915), 310(4475), 280(9920), 250(9640)	765(1945), 480(1820)
2b	610(525), 365(15575), 300(11665), 270(33385), 245(32880)	790(1215), 500(1980)
2c	605(3235), 315(7630. 290(10100), 245 (12430)	775(2255), 485(2320)
2d	515(2615), 310(4140), 285(8415), 245(10625)	800(2025), 485 (2180)
2e	560(3160), 425(3790), 335(14675), 265(32370), 250(10340)	820 (2245), 500 (2060)
2f	545(2320), 320(2680), 280(7615), 250(8110)	810(2130), 492(2200)

H_2DBC = 3,5-di-*tert*-butylcatechol.

The Mössbauer spectra of complexes **1a** and **2b** further confirm both the oxidation state (III) and high-spin state of metal center in the complex. The spectra were recorded at 80 K and show a symmetric quadruple doublet depicted in Fig. S2. This doublet accounts for 100% and 99.84% of the iron in the Mössbauer sample of **1a** and **2b**, respectively. The isomer shift and the quadruple splitting (ΔE_Q) values are 0.47 and 0.40 mms^{-1} for **1a** whereas 0.49 and 0.82 mms^{-1} for **2b** and these values are in good agreement with those reported for related high-spin iron(III) complexes [73–75].

2.4. UV–Vis spectra

The iron(III) complexes show an intense absorption band near 360 nm, which can be assigned to as the ligand to metal charge transfer transition from Cl^- to Fe(III) [39–42]. Bands around 300–315 nm may be attributed to as S(σ)–Fe(III) ligand to metal charge transfer transition [76] and the bands ~250 nm is due to

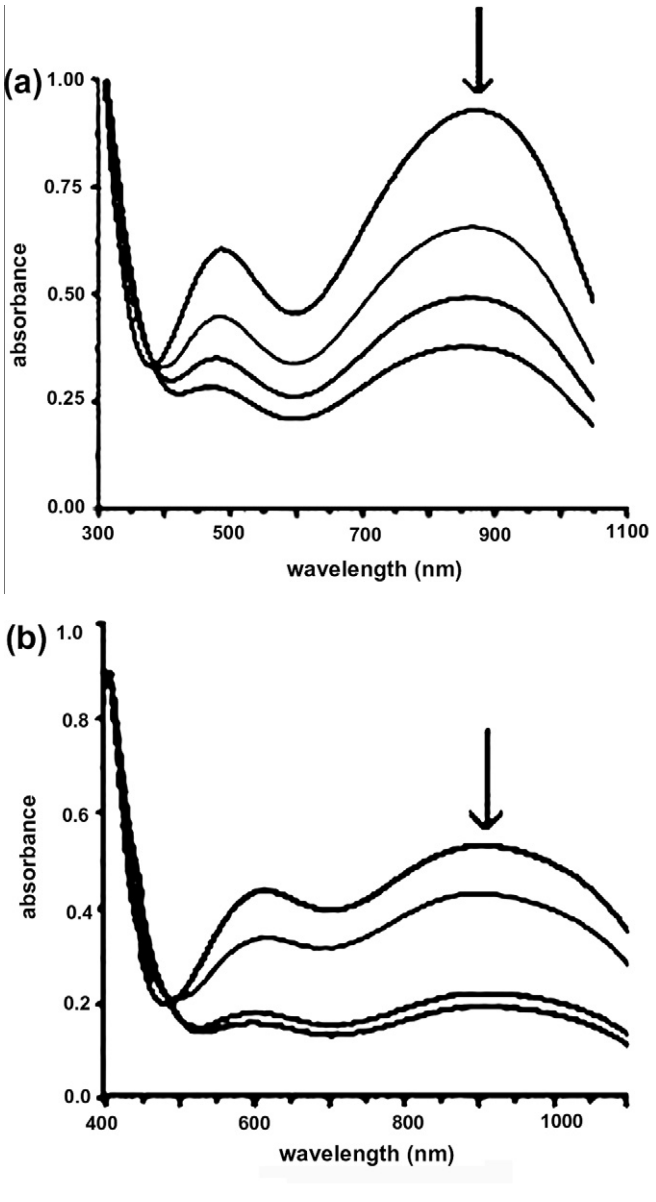

Fig. 3. Progress of the reaction of adduct [Fe(L_{SB}^1)(DBC)Cl] (a) and [Fe(L_{SB}^2)(DBC)Cl] (b) with O_2 in CH_3CN solution. The disappearance of the catecholate to iron(III) charge-transfer band was monitored.

intra-ligand transition [48]. An additional band appears as a high energy band in the region 310–350 nm for the type **2** compounds which can be assigned to the charge transfer transition from out-of-plane pπ orbital (HOMO) of the phenolate oxygen to the half filled $d_{x^2-y^2}/d_{z^2}$ orbital of iron(III). The lowest energy band (500–600 nm) in the type **2** complexes would arise from the charge transfer transition [51,77] from the in-plane pπ orbital (POMO) of the phenolate ion to the half filled d_{π^*} orbital of iron(III).

To throw light on the ability of the present complexes to interact with catechol substrates, simple and sterically hindered catechol was added to them in excess (1:1.2) to ensure complete adduct formation and their spectra were measured. Two new visible bands (480–550 nm, 750–850 nm) (Table 4) which appear on adding catechol dianions are assignable to a catecholate → Fe(III) LMCT transition, [48,24,78–80] involving two different catecholate orbitals on the chelated catecholate.

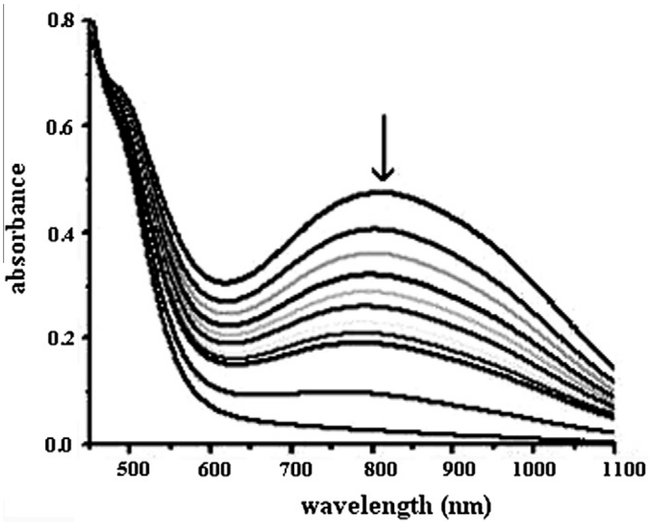

Fig. 4. Progress of the reaction of adduct [Fe(L^2)(DBC)] with O_2 in CH_3CN solution. The disappearance of the catecholate to iron(III) charge-transfer band was monitored.

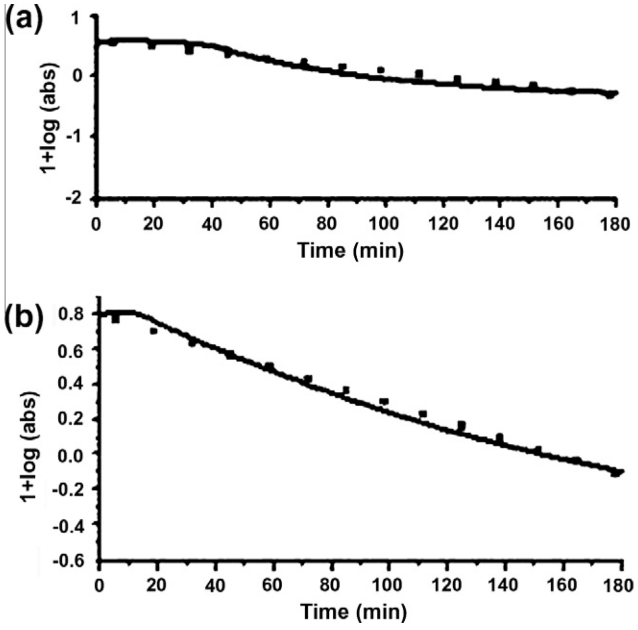

Fig. 5. Plot of [1+log(abs)] *versus* time for the reaction of [Fe($L_{SB}{}^1$)(DBC)Cl] (a) and [Fe($L_{SB}{}^2$)(DBC)Cl] (b) with O_2 in CH_3CN solution.

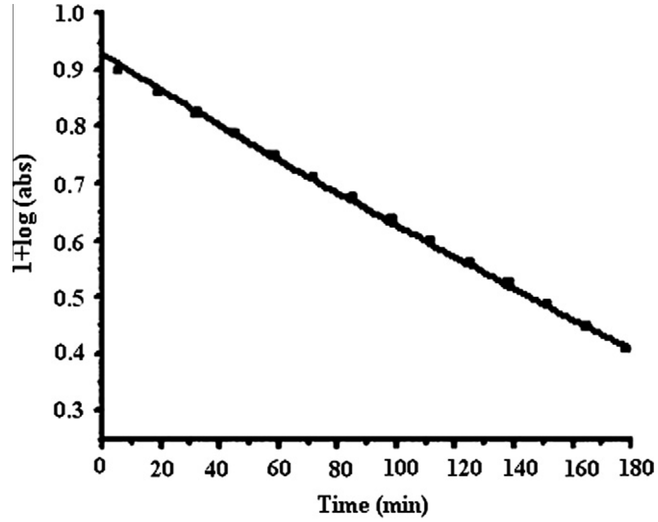

Fig. 6. Plot of [1+log (abs)] *versus* time for the reaction of [Fe(L^2)(DBC)] with O_2 in CH_3CN solution.

2.5. Catechol dioxygenase activity of iron(III) complexes

The catechol cleaving dioxygenase activity of the complexes was explored in acetonitrile solution. The catechol adducts [Fe(L_{SB})(DBC)Cl] for type **1** and [Fe(L)(DBC)] adducts for type **2** complexes were generated in situ by the addition of equimolar quantities of 3,5-di-*tert*-butylcatechol (H_2DBC) and two equivalents of piperidine and exposing the mixtures to molecular oxygen. The decomposition of complex–substrate adducts were monitored by detecting the decay of the low energy LMCT bands (Figs. 3 and 4) at ambient temperature. The oxygenated products were identified by ^1H NMR and HRMS techniques. The catecholate adducts of all the present complexes exclusively afford the intradiol cleavage products. The first step involves the binding of the 3,5-di-*tert*-butylcatecholate moiety to the iron complex as a mononuclear center and this step is assumed to be followed by the formation of substrate-alkylperoxo-Fe^{3+} intermediate [81–84] by O_2 attack which on acyl migration yields intradiol cleavage products.

The catecholase activity of the iron(III) complexes was also measured in absence of O_2 and the complexes were found to show no catecholase activity in the absence of O_2.

All the complexes were found to react with the reactants (molecular oxygen and catechol) and the oxygenation reactions exhibit pseudo-first order kinetics as judged by the linearity of the plot of [1+log(abs)] *versus* time. Plot of [1+log(abs)] *versus* time for complexes **1a** and **1b** are depicted in Fig. 5 while that for **2b** is given in Fig. 6.

Table 5
Kinetic data[a] for catalytic reaction.

Complex	k_{O2} (M^{-1} S^{-1})
[Fe^{III}($L_{SB}{}^1$)Cl_3]	9.1×10^{-3}
[Fe^{III}($L_{SB}{}^2$)Cl_3]	10.2×10^{-3}
[Fe^{III}(L^1)Cl_2]	1.29×10^{-3}
[Fe^{III}(L^2)Cl_2]	6.01×10^{-3}
[Fe^{III}(L^4)Cl_2]	1.44×10^{-3}
[Fe^{III}(L^5)Cl_2]	7.8×10^{-3}

[a] $k_{O2} = k_{obs}/[O_2]$. The solubility of O_2 in CH_3CN at 25 °C is 8.1×10^{-3} M. The kinetic data were obtained by time dependent spectral measurements for a period of 3 h.

The rate of the reaction was calculated using the equation ($k_{O2} = k_{obs}/[O_2]$) [85–87]. The value of k_{obs} is deduced from the slope of the linear graph. The rate of the reaction calculated for **1a**, **1b**, **2a**, **2b**, **2d** and **2e** are reported in Table 5. The rates are comparable with other reported complexes incorporating *O,N*-donor ligands [21,30,43,48,88,89].

Time dependent spectral measurements for **1a** and **1b** show that, **1b** reacts faster than **1a** which is due to the fact that there is an increase in positive charge on iron(III) facilitating a stronger interaction of catechols with iron(III) center. On the other hand, the rates of reaction decrease in the order **2e** > **2b** > **2d** > **2a**. Due to the bulky benzyl group, the lone pair on sulfur in **2e** is not exactly oriented towards iron causing an increase in Lewis acidity on Fe(III) center facilitating the Fe(III)–catecholate binding and hence increasing the reaction rate slightly. Furthermore, replacement of *p*–H on the phenolato ring in **2a** and **2d** by an electron withdrawing group (*–NO₂*) in **2b** and **2e** also increases the Lewis acidity on Fe(III) center enhancing the rate of the reaction.

3. Conclusion

The synthesis and structural characterization of new mononuclear iron(III) complexes incorporating *N,N,S* coordinating tridentate and a few monophenolato iron(III) complexes of new *N,N,O,S* coordinating tetradentate ligands have been isolated and studied as structural and functional models for catechol dioxygenases. As revealed by the X-ray crystal structure, the ligand is bound to the metal center in a facial coordination mode. Dioxygen cleaving catecholase activity of the complexes was carried out and all the complexes are found to be highly reactive towards intradiol cleavage of H_2DBC in the presence of dioxygen. However, in the absence of O_2, no catalytic activity has been observed. Besides this, the complexes were also characterized by UV–Vis, EPR, Mössbauer and electrochemical measurements.

4. Experimantal

4.1. Materials

All the starting materials were analytically pure and were used without further purification, and the solvents were purified by standard procedure. The ligands were prepared as described below.

4.2. Physical measurements

UV–Vis spectra were measured on a Perkin–Elmer LAMBDA 25 spectrophotometer and IR spectra were recorded with Perkin–Elmer L-0100 spectrophotometer. Electrochemical measurements were performed (acetonitrile solution) on a CHI 620A electrochemical analyzer using a platinum electrode under dinitrogen atmosphere. Tetraethylammonium perchlorate (TEAP) was used as a supporting electrolyte and the potentials are referenced to the standard calomel electrode (SCE) without junction correction. The cyclic voltammogram were recorded with a scan rate of 50 mV/s with iR compensation in all cases. X-band (9.1 GHz) EPR spectra were recorded on a Varian E-112 spectrometer at a microwave power of 1 mW and modulation amplitude of 0.5 gauss using quartz Dewar. The Dewar was filled with liquid nitrogen and the quartz sample tube was immersed in it. During the measurements, the microwave cavity was continuously purged with pure and dry nitrogen. The spectra were calibrated with respect to diphenylpicrylhydrazyl (dpph, $g = 2.0037$). Mössbauer data were recorded on alternating constant-acceleration spectrometers. The sample temperature was maintained constant in an Oxford Instruments Variox cryostat or an Oxford Instruments Mössbauer-Spectromag cryostat. The latter was used for measurement in applied magnetic fields with the field oriented perpendicular to the γ-beam. Isomer shifts are given relative to α-Fe at room temperature. Electrospray ionization mass spectra (ESI-MS) (70 eV) were recorded on a Qtof Micro YA263 spectrometer. ^1H NMR data were recorded in $CDCl_3$ solvent at 298 K with the help of Bruker 300 MHz FT spectrometer using tetramethylsilane (TMS) as an internal standard. The C, H, N content of the samples was determined with the help of a Perkin–Elmer 2400 Series II elemental analyzer.

4.3. Crystallographic studies

Single crystals of suitable quality for X-ray diffraction study of the complexes **1a** and **2b** were grown by slow evaporation of the complexes in acetonitrile solution. The X-ray intensity data were measured at 293 K on Bruker-Nonious SMART APEX CCD diffractometer (Mo Kα, $\lambda = 0.71073$ Å). The detector was placed at a distance 6.0 cm from the crystal. Total 606 frames were collected with a scan width of 0.3° in different settings of . The data were reduced in SAINTPLUS [90] and empirical absorption correction was applied using the SADABS package [90]. Metal atoms were located using direct method and the rest of the non-hydrogen atoms emerged from successive Fourier synthesis. The structures were refined by full matrix least-square procedure on F^2. All non-hydrogen atoms were refined anisotropically. The hydrogen atoms were included in calculated positions. Calculations were performed using the SHELXTL v.6.14 program package. Molecular structure plots were drawn using ORTEP [91].

4.4. Reactivity studies

The catechol cleavage activity of all of the complexes toward H_2DBC was examined by exposing the adducts [Fe(L_{SB})(DBC)Cl] and [Fe(L)(DBC)] generated in situ in CH_3CN solution to dioxygen. Kinetic analyses of the catechol cleavage reactions were carried out by time-dependent measurement of the disappearance of the lower energy LMCT bands at ambient temperature. The complexes [Fe(L_{SB})(DBC)Cl] or [Fe(L)(DBC)] (0.1 mmol) in CH_3CN solvent (5 ml) were exposed to dioxygen and stirred for 24 h. The oxygenation reaction was quenched by the addition of 6(M) HCl (5 ml). The products were extracted from the aqueous solution with CH_2Cl_2 (3 × 20 ml). The clear yellow organic layer was separated and dried over sodium sulfate. The products were subjected to column chromatography using silica gel and CH_2Cl_2/CH_3OH (8:1) mixture.

4.5. Determination of the oxidation products

The oxidation products of [Fe(L_{SB})(DBC)Cl] and [Fe(L)(DBC)] in stoichiometric reaction were analyzed by high resolution mass spectra (HRMS) and ^1H NMR techniques. After the reaction ran for 24 h, the major products were determined as intradiol cleavage products (Scheme 3) (Table 6), composed of **I**, **II** and **III**.

4.5.1. 3,5-Di-tert-butyl-5-(N,N–dimethylamidomethyl)-2-furanone (*I*)

Mass spectral data found for $C_{16}H_{27}NO_3$, $[M+Na]^+$, 303.3701; ^1H NMR (300 MHz. $CDCl_3$): 1.03(s, 9H), 1.21(s, 9H), 1.9 and 3.1(2H), 2.7(s, 6H), 6.98(s,1H) and the mass, ^1H NMR data were in agreement with literature data.

4.5.2. 3,5-Di-tert-butyl-5-(2-oxo-2-piperidinylethyl)-5H-furanone (*II*)

Mass spectral data found for $C_{19}H_{31}NO_3$, $[M+Na]^+$, 343.9416; ^1H NMR (300 MHz. $CDCl_3$): 1.00(s, 9H), 1.21(s,9H), 1.47(m, 6H), 2.74 and 2.91 (2H), 3.47(m, 4H), 7.05(s, 1H).

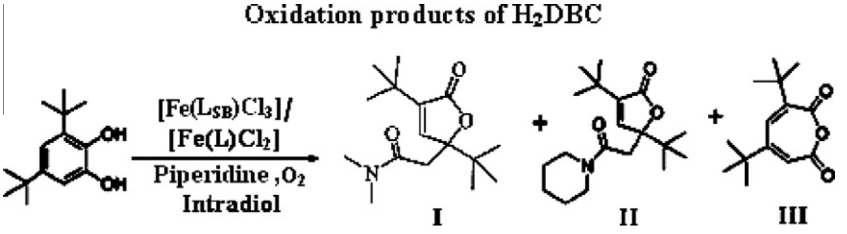

Scheme 3.

Table 6
Percentage yield of the cleavage products **I–III**.

Catechol adducts	Percentage yield
$[Fe(L_{SB}{}^1)(DBC)Cl]$	**I** (14.5), **II** (68.2), **III** (4.0)
$[Fe(L_{SB}{}^2)(DBC)Cl]$	**I** (16.4), **II** (65.5), **III** (14.0)
$[Fe(L^1)(DBC)]$	**I** (5.7), **II** (73.8), **III** (5.1)
$[Fe(L^2)(DBC)]$	**I** (5.2), **II** (66.9), **III** (4.0)
$[Fe(L^3)(DBC)]$	**I** (5.8), **II** (67.8), **III** (4.7)
$[Fe(L^4)(DBC)]$	**I** (5.5), **II** (75.1), **III** (4.2)
$[Fe(L^5)(DBC)]$	**I** (6.4), **II** (70.2), **III** (4.2)
$[Fe(L^6)(DBC)]$	**I** (6.0), **II** (72.7), **III** (3.4)

*4.5.3. 3,5-Di-tert-butyl-1-oxacyclohepta-3,5-diene-2,7-dione (**III**)*

Mass spectral data found for $C_{14}H_{20}O_3$, $[M+Na]^+$, 258.8596; ^1H NMR (300 MHz. $CDCl_3$): 1.13(s, 18H), 5.49(s, 1H), 6.43(s, 1H).

4.6. Synthesis of the ligands

The reduced Schiff bases, L_{SB}, were synthesized from the parent Schiff bases by $NaBH_4$ reduction [92] and the tripodal ligands HL were synthesized by a reported procedure [93].

*4.7. Preparation of type **1** and **2** complexes*

The $[Fe^{III}(L_{SB})Cl_3]$ and $[Fe^{III}(L)Cl_2]$ complexes were prepared by using a general method with the $FeCl_3.6H_2O$ as starting material. Details are given here for two representative cases (**1a** and **2b**).

*4.7.1. $[Fe^{III}(L_{SB}{}^1)Cl_3]$, **1a***

$L_{SB}{}^1$ (117 mg, 0.60 mmol) was added to a solution of 100 mg (0.60 mmol) of $FeCl_3{\cdot}6H_2O$ in 20 ml methanol. The reaction mixture was refluxed for 2 h producing an orange–red precipitate. It was filtered and the crystalline solid was washed thoroughly with methanol. Orange–red colored crystals were obtained by slow evaporation of the solid in acetonitrile solution. Yield: 91 mg (69%). *Anal.* Calc. for $C_{10}H_{16}Cl_3FeN_2S$: C, 33.35; H, 4.50; N, 7.76. Found: C, 33.50; H, 4.49; N, 7.81%. UV–Vis (λ_{max}/nm (ε/M^{-1} cm^{-1}) CH_3CN): 358 (4106); 309 (4474); 241 (10183). IR (KBr, cm^{-1}): ν(N–H) 3430, ν(Fe–S) 342, ν(Fe–Cl) 380. E_{pc} (Fe^{III}/Fe^{II}): −0.524 V.

*4.7.2. $[Fe^{III}(L_{SB}{}^2)Cl_3]$, **1b***

Yield: 210 mg (78%). *Anal.* Calc. for $C_{17}H_{22}Cl_3FeN_2S$: C, 42.78; H, 5.00; N, 6.61. Found: C, 42.83; H, 5.03; N, 6.66%. UV–Vis (λ_{max}/nm (ε/M^{-1} cm^{-1}) CH_3CN): 357 (2236); 313 (2985); 255 (9165). IR (KBr, cm^{-1}): ν(N–H) 3424, ν(Fe–S) 330, ν(Fe–Cl) 368. E_{pc} (Fe^{III}/Fe^{II}): −0.681 V.

*4.7.3. $[Fe^{III}(L^1)Cl_2]$, **2a***

Yield: 205 mg (80%). *Anal.* Calc. for $C_{17}H_{21}Cl_2FeN_2OS$: C, 47.56; H, 4.96; N, 6.58. Found: C, 47.68; H, 4.94; N, 6.54%. UV–Vis (λ_{max}/nm (ε/M^{-1} cm^{-1}) CH_3CN): 600(2915); 310(4474); 278(9919); 250(9639). IR (KBr, cm^{-1}): ν(C–O) 1256, ν(Fe–O) 762, ν(Fe–S) 346, ν(Fe–Cl) 452. E_{pc} (Fe^{III}/Fe^{II}): −0.22 V.

*4.7.4. $[Fe^{III}(L^2)Cl_2]$, **2b***

HL^2 (207 mg, 0.60 mmol) was added to a solution of 100 mg (0.60 mmol) of $FeCl_3{\cdot}6H_2O$ in 20 ml methanol. The reaction mixture was refluxed for 2 h producing a deep blue crystalline precipitate. It was then filtered and the crystalline solid was washed thoroughly with methanol. Deep blue colored crystals were obtained by slow evaporation of the solid in acetonitrile solution. Yield: 255 mg (89%). *Anal.* Calc. for $C_{17}H_{20}Cl_2FeN_3O_3S$: C, 43.21; H, 4.22; N, 8.89. Found: C, 43.15; H, 4.26; N, 8.88%. UV–Vis (λ_{max}/nm (ε/M^{-1} cm^{-1}) CH_3CN): 610(526); 365(15576); 300(11664); 270(33383); 245(32877). IR (KBr, cm^{-1}): ν(C–O) 1264, ν(Fe–O) 770, ν(Fe–S) 324, ν(Fe–Cl) 456. E_{pc} (Fe^{III}/Fe^{II}): −0.181 V.

*4.7.5. $[Fe^{III}(L^3)Cl_2]$, **2c***

Yield: 232 mg (83%). *Anal.* Calc. for $C_{17}H_{20}Cl_3FeN_2OS$: C, 44.18; H, 4.31; N, 6.10. Found: C, 44.18; H, 4.35; N, 6.05%. UV–Vis (λ_{max}/nm (ε/M^{-1} cm^{-1}) CH_3CN): 605(3235); 315(7631); 290(10100); 274(12428). IR (KBr, cm^{-1}): ν(C–O) 1266, ν(Fe–O) 768, ν(Fe–S) 336, ν(Fe–Cl) 481. E_{pc} (Fe^{III}/Fe^{II}): −0.186 V.

*4.7.6. $[Fe^{III}(L^4)Cl_2]$, **2d***

Yield: 245 mg (79%). *Anal.* Calc. for $C_{24}H_{28}Cl_2FeN_2OS$: C, 53.91; H, 4.68; N, 5.76. Found: C, 53.99; H, 4.72; N, 5.71%. UV–Vis (λ_{max}/nm (ε/M^{-1} cm^{-1}) CH_3CN): 515(2617); 308(4142); 285(8414); 245(10626). IR (KBr, cm^{-1}): ν(C–O) 1287, ν(Fe–O) 772, ν(Fe–S) 334, ν(Fe–Cl) 459. E_{pc} (Fe^{III}/Fe^{II}): −0.192 V.

*4.7.7. $[Fe^{III}(L^5)Cl_2]$, **2e***

Yield: 310 mg (91%). *Anal.* Calc. for $C_{24}H_{27}Cl_2FeN_3O_3S$: C, 49.33; H, 4.20; N, 7.81. Found: C, 49.37; H, 4.14; N, 7.85%. UV–Vis (λ_{max}/nm (ε/M^{-1} cm^{-1}) CH_3CN): 560(3159); 427(3792); 334(14673); 265(32371); 252(10343). IR (KBr, cm^{-1}): ν(C–O) 1290, ν(Fe–O) 764, ν(Fe–S) 330, ν(Fe–Cl) 472. E_{pc} (Fe^{III}/Fe^{II}): −0.180 V.

*4.7.8. $[Fe^{III}(L^6)Cl_2]$, **2f***

Yield: 296 mg (89%). *Anal.* Calc. for $C_{27}H_{27}Cl_3FeN_2OS$: C, 50.34; H, 4.26; N, 5.30. Found: C, 50.38; H, 4.22; N, 5.34%. UV–Vis (λ_{max}/nm (ε/M^{-1} cm^{-1}) CH_3CN): 547(2320); 320(2681); 280(7613); 249(8112). IR (KBr, cm^{-1}): ν(C–O) 1296, ν(Fe–O) 760, ν(Fe–S) 342, ν(Fe–Cl) 495. E_{pc} (Fe^{III}/Fe^{II}): −0.184 V.

Acknowledgements

Financial support from Council of Scientific and Industrial Research, New Delhi, India, Department of Science and Technology, New Delhi, India and the University Grant Commission, New Delhi are greatly acknowledged. We are also thankful to Indian Association for cultivation of Science, Kolkata, India for the data collection on the CCD facility setup.

Appendix A. Supplementary material

Supplementary data associated with this article can be found, in the online version, at doi:10.1016/j.ica.2010.05.027.

References

[1] A. Jordan, P. Reichard, Annu. Rev. Biochem. 67 (1998) 71.
[2] D.T. Logan, X.D. Su, A. Aberg, K. Regnstrom, J. Hajdu, H. Eklund, P. Nordlund, Structure 4 (1996) 1053.
[3] J. Stubbe, Curr. Opin. Chem. Biol. 7 (2003) 1053.
[4] B.C. Antanaitis, P. Aisen, Adv. Inorg. Biochem. 5 (1983) 111.
[5] A.C. Rosenzweig, C.A. Frederick, S.J. Lippard, P. Nordlund, Nature 366 (1993) 537.
[6] L. Westerheide, M. Pascaly, B. Krebs, Curr. Opin. Chem. Biol. 4 (2000) 235.
[7] A.C. Rosenzweig, X. Feng, S.J. Lippard, in: J.W. Kelly, T.O. Baldwin (Eds.), Applications of Enzyme Biotechnology, Plenum Press, New York, 1991.
[8] M. Merkx, D.A. Kopp, M.H. Sazinsky, J.L. Blazyk, J. Muller, S.J. Lippard, Angew. Chem., Int. Ed. 40 (2001) 2782.
[9] L. Shu, Y.M. Chiou, A.M. Orville, M.A. Miller, J.D. Lipscomb, L. Que Jr., Biochemistry 34 (1995) 6649.
[10] A.M. Orville, V.J. Chen, A. Kriauciunas, M.R. Harpel, E. Munck, J.D. Lipscomb, Biochemistry 31 (1992) 4602.
[11] L. Que Jr., in: T.M. Loehr (Ed.), Iron Carriers and Iron Proteins, VCH Publishers, New York, 1989, p. 467.
[12] W. Reineke, M.J. Knackmuss, Ann. Rev. Microbiol. 42 (1988) 263.
[13] M. Dekkar, in: D.T. Gibson (Ed.), Microbial Degradation of Organic Molecules, New York, 1984.
[14] L. Que Jr., J. Chem. Edu. 62 (1985) 938.
[15] L. Que Jr., R.Y.N. Ho, Chem. Rev. 96 (1996) 2607.
[16] D.H. Ohlendorf, J.D. Lipscomb, P.C. Weber, Nature 336 (1988) 403.
[17] M.W. Vetting, D.H. Ohlendorf, Structure 8 (2000) 429.
[18] M. Costas, M.P. Mehn, M.P. Jensen, L. Que Jr., Chem. Rev. 104 (2004) 939.
[19] M. Abu-Omar, A. Loaiza, N. Hontzeas, Chem. Rev. 105 (2005) 2227.
[20] T. Dhanalakshmi, M. Bhuvaneshwari, M. Palaniandavar, J. Inorg. Biochem. 100 (2006) 1527.
[21] M. Velusamy, M. Palaniandavar, G.R. Srinivasa, G.U. Kulkarni, Inorg. Chem. 42 (2003) 8283.
[22] M. Pascaly, M. Duda, F. Schweppe, F. Zurlinden, K. Muller, B. Krebs, J. Chem. Soc., Dalton Trans. (2001) 828.
[23] D.D. Cox, S.J. Benkovic, L.M. Bloom, F.C. Bradley, M.J. Nelson, L. Que Jr., D.E. Wallick, J. Am. Chem. Soc. 110 (1988) 2026.
[24] D.D. Cox, L. Que Jr., J. Am. Chem. Soc. 110 (1988) 8085.
[25] M. Pascaly, M. Duda, A. Rompel, B.H. Sift, W.M. Klaucke, B. Krebs, Inorg. Chim. Acta 291 (1999) 289.
[26] P. Mialane, L. Tehertanov, F. Banse, J. Sainton, J.J. Girerd, Inorg. Chem. 39 (2000) 2440.
[27] P. Mialane, J.J. Girerd, J. Guilhem, L. Tehertanov, Inorg. Chim. Acta 298 (2000) 38.
[28] R. Yamahara, S. Ogo, Y. Watanabe, T. Funabiki, K. Jitsukawa, H. Masuda, H. Einaga, Inorg. Chim. Acta 300 (2000) 587.
[29] X. Wang, S. Wang, L. Li, E.B. Sundberg, G.P. Gacho, Inorg. Chem. 42 (2003) 7799.
[30] M.K. Panda, A. John, M.M. Shaikh, P. Ghosh, Inorg. Chem. 47 (2008) 11874.
[31] R. Mayilmurugan, E. Suresh, M. Palaniandavar, Inorg. Chem. 46 (2007) 6038.
[32] P.K. Dhara, S. Pramanik, T.H. Lu, P. Chattopadhayay, J. Coord. Chem. 20 (2005) 985.
[33] C.A. Grapperhaus, M. Li, A.K. Patra, S. Poturovic, P.M. Kozlowski, M.Z. Zgierski, M.S. Mashuta, Inorg. Chem. 42 (2003) 4382.
[34] P. Chakraborty, S.K. Chandra, A. Chakravorty, Inorg. Chem. 33 (1994) 6429.
[35] A.J. Blake, A.J. Holder, T.I. Hyde, M.J. Schrader, Chem. Soc., Chem. Commun. (1989) 1433.
[36] T. Mashiko, C.A. Read, K.J. Haller, M.E. Kastner, W.R. Scheidt, J. Am. Chem. Soc 107 (1987) 5758.
[37] J. Mcknight, M.R. Cheesman, C.A. Reed, R.D. Orosz, A.J. Thomson, J. Chem. Soc., Dalton Trans. 15 (1991) 1887.
[38] K. Nakamoto, Infrared and Raman Spectra of Inorganic and Coordination Compounds, fourth ed., John Wiley and Sons, New York, 1986, p. 191.
[39] M.C. Rodriguez, F. Lambert, I. Morgenstern-Badarau, M. Cesario, J. Guilhem, B. Keita, L. Nadjo, Inorg. Chem. 36 (1997) 3525.
[40] D. Mandon, A. Nopper, T. Litrol, S. Goetz, Inorg. Chem. 40 (2001) 4803.
[41] K.B. Jensen, C.J. McKenzie, O. Simonsen, H. Toftlund, A. Hazell, Inorg. Chim. Acta 257 (1997) 163.
[42] H. Adams, N.A. Bailey, J.D. Crane, D.E. Fenton, J.M. Latour, J.M.J. Williams, Chem. Soc., Dalton Trans. (1990) 1727.
[43] K. Visvaganesan, R. Mayilmurugan, E. Suresh, M. Palaniandavar, Inorg. Chem. 46 (2007) 10294.
[44] K.R.J. Thomas, M. Velusamy, M. Palaniandavar, Acta Crystallogr., Sect. C., Cryst. Struct. Commun. 54 (1998) 741.
[45] A.J. Bard, L.R. Faulkner, Electrochemical Methods: Fundamentals and Applications, John Wiley and Sons, New York, 1980. p. 218.
[46] W.O. Koch, V. Schunemann, M. Gerdan, A.X. Trautwein, H.J. Kruger, Chem. Eur. J. 4 (1998) 1255.
[47] N. Raffard, R. Carina, A.J. Simaan, J. Sainton, E. Riviere, L. Tchertanov, S. Bourcier, G. Bouchoux, M. Delroisse, F. Banse, J.J. Girerd, Eur. J. Inorg. Chem. (2001) 2249.
[48] M. Velusamy, R. Mayilmurugan, M. Palaniandavar, Inorg. Chem. 43 (2004) 6284.
[49] M. Velusamy, R. Mayilmurugan, M.J. Palaniandavar, Inorg. Biochem. 99 (2005) 1032.
[50] M. Duda, M. Pascaly, B. Krebs, Chem. Commun. (1997) 835.
[51] M. Merkel, D. Schnieders, S.M. Baldeau, B. Krebs, Eur. J. Inorg. Chem. (2004) 783.
[52] M. Merkel, F.K. Muller, B. Krebs, Inorg. Chim. Acta 337 (2002) 308.
[53] M. Merkel, M. Pascaly, B. Krebs, J. Astner, S.P. Foxon, S. Schindler, Inorg. Chem. 44 (2005) 7582.
[54] R. Viswanathan, M. Palaniandavar, J. Chem. Soc., Dalton Trans. (1995) 1259.
[55] R. Viswanathan, M. Palaniandavar, T. Balasubramanian, P. Thomas Muthiah, J. Chem. Soc., Dalton Trans. (1996) 2519.
[56] M. Palaniandavar, R. Viswanathan, Proc. Indian Acad. Sci., Chem. Sci. 108 (1996) 235.
[57] E.W. Ainscough, A.M. Brodie, J.E. Plowman, K.L. Brown, A.W. Addison, A.R. Gainsford, Inorg. Chem. 19 (1980) 3655.
[58] J.C. Davis, W.S. Kung, B.A. Averill, Inorg. Chem. 25 (1986) 394.
[59] S. Yan, L. Que Jr., L.F. Taylor, O.P. Anderson, J. Am. Chem. Soc. 110 (1988) 5222.
[60] E.T. Clarke, A.E. Martell, J. Reibenspies, Inorg. Chim. Acta 196 (1992) 177.
[61] I. Malfant, I. Morgenstern-Badarau, M. Philoche-Lavisalles, F. Lloret, J. Chem. Soc., Chem. Commun. (1990) 1338.
[62] M.R. McDevitt, A.W. Addision, E. Sinn, L.K. Thompson, Inorg. Chem. 29 (1990) 3425.
[63] R. Viswanathan, M. Palaniandavar, T. Balasubramanian, P. Thomas Muthiah, Inorg. Chem. 37 (1998) 2943.
[64] M. Velusamy, M. Palaniandavar, R. Srinivasagopalan, G.U. Kulkarni, Inorg. Chem. 37 (2003) 2943.
[65] R.B. Lauffer, R.H. Heistand, L. Que Jr., Inorg. Chem. 22 (1983) 50.
[66] L. Casella, M. Gullotti, A. Pintar, L. Messori, A. Rockenbauer, M. Gyorl, Inorg. Chem. 26 (1987) 1031.
[67] M.I. Scullane, L.K. White, N. Chasteen, J. Magn. Reson. 47 (1982) 383.
[68] W.T. Oosterhuis, Struct. Bonding (Berl.) 20 (1974) 59.
[69] G. Lang, R. Aasa, K. Garbett, R.J.P. Williams, J. Chem. Phys. 55 (1971) 4539.
[70] R.J. Aasa, Chem. Phys. 52 (1970) 3919.
[71] R. Singh, C. de Graaf, E. Colacio, K.K. Rajak, Polyhedron 27 (2008) 2751.
[72] M. Ray, R. Mukherjee, J.F. Richardson, R.M. Buchanan. J. Chem. Soc., Dalton Trans. (1993) 2451.
[73] C. Brewer, G. Brewer, R.J. Butcher, E.E. Carpenter, L. Cuenca, B.C. Noll, W.R. Scheidt, C. Viragh, P.Y. Zavalij, D. Zielaski, Dalton Trans. (2006) 1009.
[74] Y. Maeda, H. Oshio, K. Toriumi, Y. Takashima, J. Chem. Soc., Dalton. Trans. (1991) 1227.
[75] T.C. Gibb, N.N. Greenwood, in: Mössbauer Spectroscopy, Chapman and Hall, London, 1971; pp 148.
[76] R. Balamurugan, M. Palaniandavar, H. Stoeckli-Evans, M. Neuburger, Inorg. Chim. Acta 359 (2006) 1103.
[77] M.I. Davis, A.M. Orville, F. Neese, J.M. Zaleski, J.D. Lipscomb, E.I.J. Solomon, Am. Chem. Soc. 124 (2002) 602.
[78] S. Salama, J.D. Stong, J.B. Neilands, T.G. Spiro, Biochemistry 17 (1978) 3781.
[79] W. Koch, H.J. Kruger, Angew. Chem., Int. Ed. Engl. 36 (1997) 1342.
[80] J.H. Lim, H.J. Lee, K.B. Lee, H.G. Jang, Bull. Korean Chem. Soc. 18 (1997) 1166.
[81] M.Y.M. Pau, M.I. Davis, A.M. Orville, J.D. Lipscomb, E.I. Solomon, J. Am. Chem. Soc. 129 (2007) 1944.
[82] M.Y.M. Pau, J.D. Lipscomb, E.I. Solomon, Proc. Natl. Acad. Sci. USA 104 (2007) 18355.
[83] G. Lin, G. Reid, T.D.H. Bugg, J. Am. Chem. Soc. 123 (2001) 5030.
[84] E.G. Kovaleva, J.D. Lipscomb, Science 316 (2007) 453.
[85] W.O. Koch, H.J. Kruger, Angew. Chem., Int. Ed. Engl. 34 (1995) 2671.
[86] Kagaku-Binran Basic Part II, second ed., Japan Chemical Society, Maruzen, Tokyo, 1975.
[87] D.T. Sawyer, Oxygen Chemistry, Oxford University Press: New York, 1991.
[88] F. Li, M. Wang, P. Li, T. Zang, L. Sun, Inorg. Chem. 46 (2007) 9364.
[89] R. Yamahara, S. Ogo, H. Masuda, Y. Watanabe, J. Inorg. Biochem. 88 (2002) 284.
[90] SMART, SAINT, SADABS, XPREP, SHELXTL, Bruker AXS Inc., Madison, WI, 1998.
[91] C.K. Johnson, ORTEP, Report ORNL-5138, Oak Ridge National Laboratory, Oak Ridge, TN, 1976.
[92] S. Larsen, K. Michelsen, E. Pedersen, Acta Chem. Scan. Sect. A 40 (1986) 63.
[93] K. Kannappan, R. Mahalakshmy, T.M. Rajendiram, R. Venkatesan, P. Sambasiva Rao, Proc. Indian Acad. Sci. (Chem. Sci.) 115 (2003) 1.